Materials Science & Engineering A 731 (2018) 21–28

Contents lists available at ScienceDirect

Materials Science & Engineering A

journal homepage: www.elsevier.com/locate/msea

Effect of boron on the tensile and creep properties of a newly developed Ni-Fe-based weld metal

Dong Wu[a,b], Tingting Yao[c], Dianzhong Li[c], Shanping Lu[a,c,*]

[a] CAS Key Laboratory of Nuclear Materials and Safety Assessment, Institute of Metal Research, Chinese Academy of Sciences, China
[b] University of Chinese Academy of Sciences, Beijing 100049, China
[c] Shenyang National Laboratory for Materials Science, Institute of Metal Research, Chinese Academy of Sciences, Shenyang 110016, China

ARTICLE INFO

Keywords:
Solidification microstructure
Secondary ion mass spectrometry (SIMS)
Grain boundary Segregation
Mechanical properties
Superalloy
Electron energy loss spectroscopy (EELS)

ABSTRACT

Boron in Ni-Fe-based weld metals exists in a state of segregation at the grain boundaries and as a solid solution in the matrix. Boron segregation increased the tensile and creep ductility at 700 °C by suppressing intergranular failure. Moreover, B-doped weld metals exhibited longer rupture lives and lower steady creep rates. However, these improvements disappeared during exposure to 700 °C within 2000 h, which was mainly attributed to a change in boron distribution from segregation at the grain boundaries to incorporation in M_2B-type borides. The electron energy loss spectroscopy results indicated that boron did not diffuse into the $M_{23}C_6$ carbides.

1. Introduction

For fulfilling the requirement of higher efficiency and lower pollution in the advanced ultra-supercritical (A-USC) power plants, the steam temperature of 700–760 °C and above in the A-USC boiler are being pursued [1,2]. In this case, the currently used ferrite [3] and austenitic steels [4] cannot attach the requirement of the long term rupture strength (100 MPa for 10^5 h) at the service temperature [2]. Ni-based superalloys such as Inconel 617B [5], Haynes 282 [6] and Inconel 740H [7] have been in development and considered as promising candidates for the application in the hottest components of the boilers in the A-USC power plants due to their excellent creep-rupture resistances and corrosion resistances at serving temperature. Recently, a Ni-Fe-based alloy, GH984, is designed for the boiler components in the A-USC power plants [8]. It attracts much attention for not only its excellent workability and low costs but also its good serving-temperature performance [9,10]. At present, alloy GH984 and its corresponding Ni-Fe-based welding materials which are developed for the invariable requirement of welding application in the A-USC plant are under development [11–13].

It is generally accepted that adding an appropriate amount of boron to superalloys is beneficial for their creep-rupture resistances [14,15]. GH984 alloy, for instance, increased 139% (from 115 to 275 h) and 178% (from 14% to 39%)in rupture life and elongation, respectively, at 700 °C and 350 MPa by adding 60 ppm boron [10]. However, the exact role of boron in superalloys is debated and a variety of possible strengthening mechanisms have been described. Boron is mostly considered to form covalent bonds at the grain boundaries, thereby increasing boundary cohesion and inhibiting embrittlement [16,17]. It has also been claimed that boron decreases the rate of void formation by decreasing grain boundary diffusivity, thus enhancing creep resistance [18,19]. In addition, some studies have proposed a softening mechanism of boron easing dislocation movement at grain boundaries, thereby lessening the tendency for crack nucleation [20,21]. It has also been proposed that boron may modify microstructures, such as the agglomeration of $M_{23}C_6$ carbides at grain boundaries [10,22] or serration of grain boundaries [23,24], which may reduce crack propagation. From this, segregation of boron at grain boundaries seems required for achieving beneficial effects. In addition to the above, boron incorporation into borides [25–27] or carbides [28,29] has also been reported. For instance, Thuvander and Stiller [27] studied the effect of boron addition to a model Ni-30 Cr-10 Fe alloy and showed that solid dissolved boron was incorporated into M_2B-type borides upon aging at 700 °C. Similar results obtained by Kurban et al. [28] showed that boron was incorporated into $M_{23}C_6$ at the grain boundaries during aging at 800 °C in alloy 304. Thus, the distribution of boron in alloys changes with the thermal process. However, the influence of the thermal process on the boron distribution has rarely been further examined in terms of the evolution of mechanical properties in alloys. Moreover, the influence of boron on the weld metal of GH984 superalloy, which is significant for the chemical composition design, have not been studied before. Thus, effects of boron addition to the Ni-Fe-based alloy on weld metal are studied for the first time in our work. In the present paper, Ni-Fe-based filler wires without boron and boron

* Corresponding author at: CAS Key Laboratory of Nuclear Materials and Safety Assessment, Institute of Metal Research, Chinese Academy of Sciences, China.
E-mail address: shplu@imr.ac.cn (S. Lu).

https://doi.org/10.1016/j.msea.2018.06.027
Received 3 February 2018; Received in revised form 7 June 2018; Accepted 7 June 2018
Available online 08 June 2018
0921-5093/

Table 1
Chemical compositions of the Ni-Fe alloy investigated in this work (wt%).

Alloy	B	C	Fe	Cr	Ti + Al	Mo	Nb	Ni
B0 (B free)	< 0.0005	0.047	20.6	19.51	1.89	2.22	1.19	Bal.
B50 (50 ppm B)	0.005	0.043	20.0	19.63	1.94	2.25	1.19	

Table 2
Main parameters of the gas tungsten arc welding (GTAW) process.

Current	180 A
Voltage	14 V
Welding speed	0.1 m/min
Wire feeding rate	1 m/min
Protective atmosphere	99.999% Ar 15 L/min
Interpass temperature	50–70 °C

doped (50 ppm B) were prepared to study the effects of boron on the microstructural and mechanical properties of the weld metal during long-term exposure at 700 °C.

2. Experimental procedures

Two Ni-Fe-based filler wires, both 1.2 mm in diameter, were produced by cold drawing and had compositions as shown in Table 1. Gas tungsten arc welding (GTAW) was used for preparing the weld metals, with the main welding parameters shown in Table 2. The base metals for welding were also prepared from the GH984 superalloy to eliminate dilution. The dimensions of base metal and backing plate were 350 mm × 150 mm × 12 mm and 400 mm × 20 mm × 12 mm respectively. The weldment design and the sizes of the mechanical-test specimens were shown in Fig. 1. After welding, the weld metals were subjected to a standard aging treatment of 8 h at 750 °C followed by water cooling which is identical to the standard aging treatment for the GH984 superalloy [10], and subsequent long-term exposure of up to 5000 h at 650 or 700 °C followed by water cooling.

Electron microscopy was performed on the samples with a Supra 35 scanning electron microscope (SEM) and FEI Tecnai20 transmission electron microscope (TEM). Bulk samples for SEM observation were prepared via mechanical polishing followed by electroetching in 10 g oxalic acid plus 90 mL H_2O. TEM foils were mechanically thinned to 50–60 μm and electropolished using a 10% perchloric acid methanol

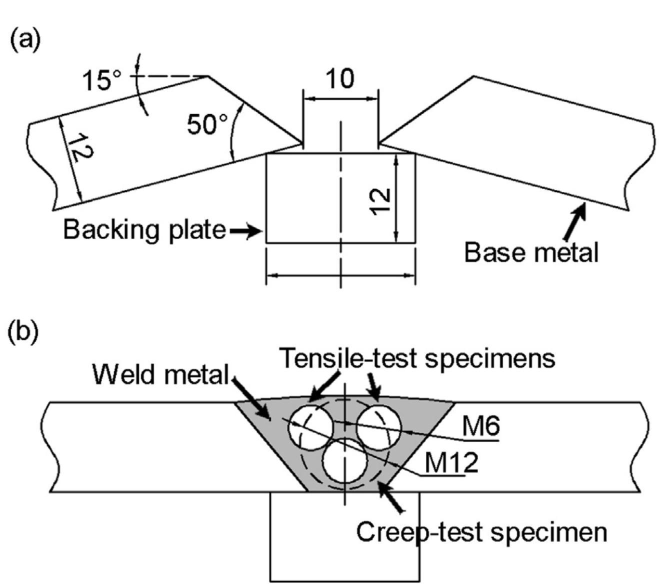

Fig. 1. Schematics showing the (a) groove design and (b) location of mechanical-test specimens in the weld metal.

solution at − 25 °C and 25 V. Secondary ion mass spectrometry (SIMS) analysis was carried with ION-TOF SIMS V (ION TOF) after the samples were ion milled for 40 min to minimize the strained layer and contamination rate. SIMS was performed at 30 keV and 1.0 pA with Bi_1^+ as the ion source in our study. SIMS ion images showing the boron and chromium distributions were acquired using $^{11}B^+$ and $^{52}Cr^+$ ions, respectively. To identify the B and C elements in the precipitates, electron energy loss spectroscopy (EELS) was conducted with an aberration-corrected FEI Titan cubed G2 60–300 S/TEM operating at 300 kV.

Tensile tests were performed at 650 and 700 °C in air with heat retention for 10 min. The strain rates were approximately 8.3×10^{-6} s^{-1} up to yield and 8.3×10^{-5} s^{-1} after yield under displacement control. Three tensile samples were measured for each condition. Creep tests were conducted in air at 700 °C and 380 or 250 MPa. All specimens for mechanical testing were cut out of the all-weld metals along the welding direction.

3. Result and discussion

3.1. Characterization of boron

At least two 150 μm × 150 μm fields of view were analyzed by SIMS for each condition of the B50 alloy (with 50 ppm boron). Fig. 2(a), (c), (e), (g) shows the SIMS results illustrating the boron distributions for each heat treatment condition at 700 °C using different exposure times (i.e., holding times). Continuous traces of boron distributed along the grain boundaries in the as-welded (AW) and standard-aged (SA) conditions (see Fig. 2(a) and (c), respectively) indicate that boron segregated significantly at the grain boundaries; in addition, boron also solid dissolved in the matrix. After exposure at 700 °C for 2000 h, more dispersive dots with high B intensity were detected (see Fig. 3(e)). Simultaneously, the signal for the continuous B traces along the grain boundaries weakened. When the exposure time was extended to 5000 h (see Fig. 2(g)), B was no longer distributed precisely along the grain boundaries, which indicates that B was gradually incorporated into second phases during exposure at 700 °C. From the SIMS images, it also can be seen that the matrix concentration of boron after exposure was lower than that in the AW and SA conditions, which can be attributed to the formation of B-containing phases.

Typical SEM images of the grain boundaries in the B50 weld metals in different conditions corresponding to the SIMS images are shown in Fig. 2(b), (d), (f) and (h). It can be seen that the grain boundaries are free of second phases in the AW condition(see Fig. 2(b)), while discrete phases nucleated and precipitated along the grain boundaries in the SA condition(see Fig. 2(d)). These precipitates grew into continuous networks at the grain boundaries gradually during the thermal exposure process(see Fig. 2(f) and (h)). The TEM and selected-area diffraction (SAD) analyses (see Fig. 3(a)) of samples exposed to 700 °C for 2000 h reveal that the grain boundaries were mainly decorated by $M_{23}C_6$ carbides, and that these particles had a coherent $[110]_{\gamma/\gamma'}//[110]_{M23C6}$ relationship with the γ/γ' matrix. This has also been reported in many other studies on this kind of Ni-Fe-based alloy [8,30,31]. Due to the uniform coherent relationship the $M_{23}C_6$ carbides grew and formed continuous grain-boundary films during the thermal treatments as shown in Fig. 2(d), (f) and (h).

In addition, a kind of face-centered orthorhombic M_2B-type boride can be observed at the grain boundaries and interiors in the samples exposed to 700 °C for 2000 h, as determined by analytical TEM in Fig. 3(b)-(d). M_2B-type boride contained a high density of stacking faults, as shown in Fig. 3(b). From Fig. 3(c) and (d), the lattice parameters were determined to be a = 1.561 nm, b = 0.804 nm, and c = 0.443 nm, values that are similar to those reported by Hu et al. [32]. The acquired EELS spectra of $M_{23}C_6$ carbide and M_2B boride are presented in Fig. 3(e) and (f), with core-loss edges of C-K and B-K, respectively. It can be seen that boron did not enter $M_{23}C_6$ and was only detected in M_2B. Many researchers have studied the effects of heat